Obliquely Incident Poincaré Waves on a Sloping Continental Shelf

PRITHA DAS AND JASON H. MIDDLETON

Department of Applied Mathematics, The University of New South Wales, Sydney, Australia

(Manuscript received 6 May 1996, in final form 19 November 1996)

ABSTRACT

An analytical theory of barotropic tides propagating onto a sloping continental shelf from the deep ocean is developed. The plane Poincaré waves incident from the deep ocean are obliquely angled, and a full matching of shelf and ocean solutions is implemented. Allowance for a nonzero water depth at the coast requires an additional term, the Bessel function of second kind, in the solution. The full solution is examined for response characteristics for both frictionless tides and for tides affected by a linear bottom friction, and energy dissipation rates are evaluated. Results for narrow continental shelves indicate that a small but nonzero coastal wall depth, in conjunction with the angle of incidence, can play a significant role in modifying the response, while for wider continental shelves both of these features greatly modify the response at resonance.

1. Introduction

Tides have fascinated men from earliest times. The modern theory of tide is founded on Newton's theory of gravitation and Euler's equations of motion. Laplace combined these together and formed the governing equations for the mathematical study of tides, which are known as the Laplace tidal equations. In shallow coastal waters the effect of gravitational forces on the response is small compared with that of the deep ocean tide, and bottom friction plays an important role in energy dissipation.

A number of theoretical studies of tides propagating onto a continental shelf have been published. Interest has centered around the factors affecting amplification, particularly near resonant conditions, and energy dissipation rates. Two types of approaches have been made. Webb (1976), Buchwald (1980), and Middleton and Bode (1987) considered a flat-bottom shelf of constant depth and were able to determine an exact solution by matching with the deep ocean to predict the tide height, currents, and dissipation of energy on the shelf. By contrast Clarke and Battisti (1981), Battisti and Clarke (1982a,b), and Church et al. (1985) have taken a constant slope approach (with the depth at the coast taken to be zero), but they did not match shelf and deep ocean solutions. On the other hand, they used coastal observation data to predict shelf tides and currents.

Webb (1976) calculated the tidal response of the Patagonian continental shelf. In his model he considered a Kelvin wave propagating along a canal, with a rectangular continental shelf at the end. He showed that maximum incident energy was absorbed at resonance. Buchwald (1980) simplified Webb's problem by replacing the Kelvin wave by a normally incident Poincaré wave and showed that this absorption was maximized at a particular value of the friction parameter, which depends on the shelf geometry. Middleton and Bode (1987) adapted Buchwald's model to include an obliquely incident Poincaré wave. They concluded that the response depends on the angle of incidence, and that left and right bounded waves behave differently. The angle of incidence plays an important role in determining the dissipation rate of tidal energy on the shelf and the magnitude and frequency of resonant peaks.

Clarke and Battisti (1981) and Battisti and Clarke (1982a,b) have investigated tides on a smoothly sloping shelf where longshore variations in coastline and topography are on a much larger scale than the width of the continental shelf. From a knowledge of the coastal data they predicted offshore shelf tides and currents. They did not consider explicitly the effects of oblique incidence. No calculations were made to determine the dissipation of tidal energy on the shelf. They considered a sloping shelf but they did not take into account a possible nonzero depth at a coastal wall. Their theories are less applicable for a very wide shelf or for shelves having slope less than 10^{-3}, where important additional terms are neglected. Church et al. (1985) used a model similar to that of Battisti and Clarke (1982a) to predict the currents in the central Great Barrier Reef. Koblinsky (1981) developed a one-dimensional numerical model to predict the tidal sea level and current amplitudes

Corresponding author address: Dr. Jason H. Middleton, Department of Applied Mathematics, The University of New South Wales, 2052 Sydney, Australia.
E-mail: j.middleton@unsw.edu.au

across the West Florida shelf from the coastal sea level and the cross-shelf topography.

A major aim of this paper is to determine the effects on tidal response of having a coastal wall of nonzero depth and an oblique angle of incidence. The inclusion of a coastal wall in the model allows for situations where the increase in depth at the coast is relatively steep but not necessarily vertical. This can occur in areas of coastal cliffs, or simply when the increase in depth occurs over a distance much smaller than the shelf width. Reference to a range of navigational charts shows that these features are not uncommon.

In this paper we have considered tides on a linear slope having a finite depth at the coast driven by incident Poincaré waves, which impinge at an angle to the shelf. Ocean–shelf matching allows calculation of the dissipation of tidal energy on the shelf. To keep the problem tractable it is assumed that there is no alongshelf dependence of the shelf profile and that the alongshelf scale of the tides on the shelf is much larger than the width of the shelf (Clarke 1991). We have also ignored effects due to alongshore variations in the amplitude of the incident tide.

In this paper, section 2 considers the formulation of the problem and its solution. Section 3 represents results both for zero and nonzero shelf friction. Section 4 summerizes the results with a discussion.

2. The model

a. Formulation of the problem

The model geometry of our problem is shown in Fig. 1, which represents a sloping continental shelf where depth h is a function of offshore coordinate x. Poincaré waves are incident at an angle α at the shelf break, h_1 and h_2 represent the depth at the coast and at the shelf break, and h_o represents the depth of the deep ocean.

The depth-averaged, unforced, linearized, inviscid equations of motion for a barotropic tidal flow in a rotating medium are given by

$$u_t - fv = -g\eta_x + \frac{1}{\rho h}X \tag{1}$$

$$v_t + fu = -g\eta_y + \frac{1}{\rho h}Y \tag{2}$$

$$\eta_t + (hu)_x + (hv)_y = 0, \tag{3}$$

where (u, v) are the depth-averaged velocities in the x direction (cross shelf) and y direction (alongshore) respectively, f is the Coriolis parameter, g is the acceleration due to gravity, η is the surface elevation, ρ is the density of water, X and Y are the bottom stresses in the x and y direction, z is the distance up from the sea surface, and h is the water depth.

Bottom stress can be linearized as (Battisti and Clarke 1982a)

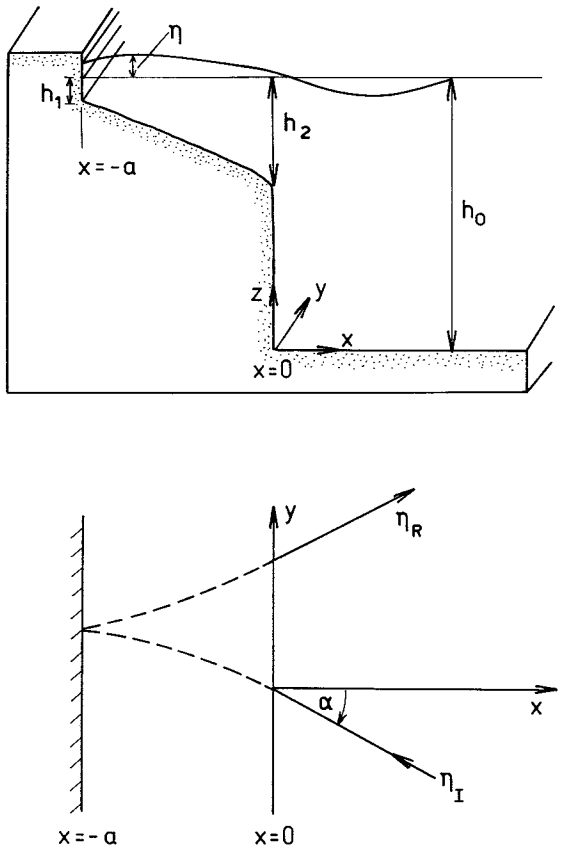

FIG. 1. Schematic diagram showing Poincaré waves obliquely incident to a sloping continental shelf. Here h_1 denotes the depth at the coast, h_2 the depth at the shelf break, h_o the depth of the deep ocean, and η is the surface elevation.

$$X = -\rho r_1 u$$

$$Y = -\rho r_1 v,$$

where $r_1(x) = c_D|\underline{u}|$. Here c_D is the drag coefficient and $|\underline{u}|$ is the root-mean-square velocity of higher frequencies motions. Then Eqs. (1) and (2) reduce to

$$u_t - fv = -g\eta_x - \frac{r_1 u}{h} \tag{4}$$

$$v_t + fu = -g\eta_y - \frac{r_1 v}{h}. \tag{5}$$

Since $r_1(x)/h(x)$ vary slowly across the shelf, setting $r_1/h = \text{const} = r/h_a$ where r is a constant friction coefficient and h_a is the average depth on the shelf, is a reasonable approximation (Battisti and Clarke 1982a). Under these approximations the depth-averaged, linearized shallow-water equations appropriate for tidal motion become

$$u_t - fv = -g\eta_x - \frac{ru}{h_a} \tag{6}$$

$$v_t + fu = -g\eta_y - \frac{rv}{h_a}. \tag{7}$$

For tidal motion of the form $\exp(i\omega t)$, $\partial/\partial t$ can be replaced by $i\omega$, and so from (6) and (7)

$$\left(i\omega + \frac{r}{h_a}\right)u - fv = -g\eta_x \tag{8}$$

$$\left(i\omega + \frac{r}{h_a}\right)v + fu = -g\eta_y. \tag{9}$$

Let

$$\sigma = \omega\left(1 - \frac{ir}{\omega h_a}\right), \tag{10}$$

then (8) and (9) reduce to

$$i\sigma u - fv = -g\eta_x \tag{11}$$

$$i\sigma v + fu = -g\eta_y. \tag{12}$$

Using (11) and (12) the velocities are found to be

$$u = \frac{g}{\sigma^2 - f^2}(i\sigma\eta_x + f\eta_y) \tag{13}$$

$$v = \frac{g}{\sigma^2 - f^2}(i\sigma\eta_y - f\eta_x). \tag{14}$$

b. Tides in the deep ocean

Velocities in the deep ocean [where $r/(\omega h_a) \ll 1$] are found by putting $h_a = h_o$, $r = 0$, and $\sigma = \omega$ in (13) and (14), so

$$u_o = \frac{g}{\omega^2 - f^2}(i\omega\eta_x + f\eta_y) \tag{15}$$

$$v_o = \frac{g}{\omega^2 - f^2}(i\omega\eta_y - f\eta_x). \tag{16}$$

Substituting (15) and (16) into (3) gives

$$\frac{\partial^2\eta}{\partial x^2} + \frac{\partial^2\eta}{\partial y^2} + \frac{\omega^2 - f^2}{gh_o}\eta = 0. \tag{17}$$

Assuming an incident and reflected wave in the deep ocean of the form

$$\eta_I = Ie^{i(k_o x + ly + \omega t)} \tag{18}$$

$$\eta_R = Re^{i(-k_o x + ly + \omega t)} \tag{19}$$

and substituting into (17) using $\eta = \eta_I + \eta_R$ gives the dispersion relation for the deep ocean as

$$\kappa^2 = k_o^2 + l^2 = \frac{\omega^2 - f^2}{gh_o}. \tag{20}$$

The angle of incidence of the obliquely incident wave may be defined as

$$\tan\alpha = \frac{-l}{k_o} \tag{21}$$

as in Middleton and Bode (1987). The seaward velocity just beyond the shelf edge is found from (15) to be

$$u_o = \frac{\omega k_o g}{\omega^2 - f^2}\left[(R - I) + i\frac{fl}{\omega k_o}(R + I)\right]e^{i(ly + \omega t)}. \tag{22}$$

c. Tides on a sloping shelf

The topography of a sloping shelf may be given by

$$h(x) = \begin{cases} h_1 + s(x + a), & -a \le x \le 0 \\ h_o, & x > 0. \end{cases} \tag{23}$$

Equation (23) represents a shelf region of uniform slope with a drop of h_1 at the coast ($x = -a$) and a perpendicular drop off at $x = 0$ to a deep sea region ($x > 0$) of constant depth h_o. For simplicity of notation we define

$$h_2 = h_1 + sa.$$

Noting $h = h(x)$ and $g/(\sigma^2 - f^2)$ is a constant from the definition of σ, substitution of (13) and (14) into (3) gives the full governing equation for sea level on the sloping shelf as

$$\eta_{xx} + \eta_{yy} + \frac{h_x}{h}\eta_x + \frac{h_x}{h}\frac{f}{i\sigma}\eta_y + \frac{\sigma^2 - f^2}{i\sigma gh}i\omega\eta = 0.$$

From (18) and (19) the alongshore dependence is given by

$$\eta_y = il\eta, \tag{24}$$

so the above expression simplifies to

$$\eta_{xx} + \frac{h_x}{h}\eta_x + \left[-l^2 + \frac{h_x}{h}\frac{fl}{\sigma} + \frac{\omega(\sigma^2 - f^2)}{\sigma gh}\right]\eta = 0. \tag{25}$$

Since we are considering only those continental margins whose significant bends in the coastline have a scale much larger than the shelf width (i.e., both the alongshore tidal scale l^{-1} and the alongshore scale of coastline bends is much larger than the shelf width), the l^2 term in (25) can be neglected (Clarke and Battisti 1981). Neglecting l^2 and using (23), the above expression (25) simplifies to

$$h^2\eta_{hh} + h\eta_h + h\mu\eta = 0, \tag{26}$$

where the complex constant μ is given by

$$\mu = \frac{fl}{\sigma s} + \frac{\omega(\sigma^2 - f^2)}{\sigma g s^2}. \tag{27}$$

Substituting $z^2 = 4\mu h$, the above equation (26) simplifies to a Bessel equation of zero order and its solution is given by

$$\eta_s(z) = [C_1 J_o(z) + C_2 Y_o(z)]e^{i(ly + \omega t)}. \tag{28}$$

Here C_1 and C_2 are constants to be determined from the boundary conditions. We note in the following that

$$\frac{\partial J_o}{\partial z} = -J_1(z); \qquad \frac{\partial Y_o}{\partial z} = -Y_1(z)$$

and also that

$$\frac{\partial}{\partial x} = \frac{2\mu s}{z}\frac{\partial}{\partial z}.$$

The relation between the two constants C_1 and C_2 can be found from the boundary condition at the coast, that is, $u = 0$ at $x = -a$. This condition constrains η_s by

$$(\eta_s)_x = -\frac{fl}{\sigma}\eta_s \qquad \text{at } x = -a. \tag{29}$$

For simplicity of expression, let us define

$$z = \begin{cases} z_1, & x = -a \\ z_2, & x = 0. \end{cases} \tag{30}$$

From (29) the coastal condition gives

$$\frac{C_1}{C_2} = \frac{\gamma z_1 Y_o(z_1) - Y_1(z_1)}{J_1(z_1) - \gamma z_1 J_o(z_1)} = \tau \qquad \text{(say)}. \tag{31}$$

Thus τ is a complex constant that depends on the parameter γ, which is defined as

$$\gamma = \frac{fl}{2\sigma\mu s}. \tag{32}$$

d. Matching ocean and shelf solutions

The offshore component of velocity u_s at the shelf break is found through (13) to be

$$u_s = \frac{ig\sigma C_2}{\sigma^2 - f^2} 2\mu s \left[-\frac{1}{z_2}\{\tau J_1(z_2) + Y_1(z_2)\} + \gamma\{\tau J_o(z_2) + Y_o(z_2)\} \right] e^{i(ly+\omega t)}. \tag{33}$$

Now C_2 can be determined from the boundary conditions at the shelf break; that is, hu and η must be continuous at the shelf break. This implies that at $x = 0$

$$\eta_s = \eta_I + \eta_R \tag{34}$$

$$u_s h_s = u_o h_o. \tag{35}$$

These give

$$C_2[\tau J_o(z_2) + Y_o(z_2)] = I + R \tag{36}$$

and

$$C_2\left[\tau\left(\gamma J_o(z_2) - \frac{1}{z_2}J_1(z_2)\right) + \gamma Y_o(z_2) - \frac{1}{z_2}Y_1(z_2)\right] = G\left[(R - I) + i\frac{fl}{\omega k_o}(R + I)\right], \tag{37}$$

where γ is given by (32) and

$$G = \frac{1}{i}\frac{h_o}{h_2}\frac{\omega(\sigma^2 - f^2)}{\sigma(\omega^2 - f^2)}\frac{k_o}{2s\mu}. \tag{38}$$

Equations (36) and (37) can be manipulated to give

$$C_2 = \frac{2I}{\Delta}, \tag{39}$$

where

$$\Delta = \frac{1}{G}\left[(\tau J_o(z_2) + Y_o(z_2))\left\{G\left(1 + i\frac{fl}{\omega k_o}\right) - \gamma\right\} + \frac{1}{z_2}(\tau J_1(z_2) + Y_1(z_2))\right]. \tag{40}$$

Therefore η on the shelf is given by

$$\eta_s = C_2[\tau J_o(z) + Y_o(z)]. \tag{41}$$

Several ratios are useful for describing the tidal response under differing conditions. First, the ratio of the amplitude of the reflected and incident wave is

$$\frac{|R|}{I} = \frac{|\eta_o|}{I} - 1. \tag{42}$$

The tidal amplification at the coast compared to the incident wave amplitude in the deep ocean is given by

$$\frac{|\eta_c|}{I} = \frac{|C_2|[|\tau J_o(z_1) + Y_o(z_1)|]}{I}. \tag{43}$$

The ratio of tidal height on the shelf to the that at the shelf break is given by

$$\frac{|\eta_s|}{|\eta_o|} = \frac{|\tau J_o(z) + Y_o(z)|}{|\tau J_o(z_2) + Y_o(z_2)|}, \tag{44}$$

and the ratio $|\eta_c|/|\eta_o|$ is given by (44) with $z = z_1$.

Dissipation D has been calculated following Middleton and Bode (1987) and is given by

$$D = \frac{1}{2}\rho g(gh_o)^{1/2}(1 - f^2/\omega^2)^{-1/2}(I^2 - |R|^2)\cos\alpha, \tag{45}$$

and the normalized dissipation D_n is

$$D_n = (1 - f^2/\omega^2)^{-1/2}(I^2 - |R|^2)\cos\alpha. \tag{46}$$

Another important ratio is that of the alongshore current $v_s(x)$ to the offshore current $u_s(x)$ on the shelf:

$$\frac{|v_s(x)|}{|u_s(x)|} = \frac{|\sigma lzA + 2f\mu sB|}{|flzA - 2\sigma\mu sB|}, \tag{47}$$

where A and B are given by

$$A = \tau J_o(z) + Y_o(z) \text{ and } B = \tau J_1(z) + Y_1(z). \tag{48}$$

e. Ray tracing when z *is large*

To examine the behavior of the solution when z is large let us put $C_2 = -iC_3$ in (28). Then

$$\eta_s(z) = [C_1 J_o(z) - iC_3 Y_o(z)]\, e^{i(ly+\omega t)}. \quad (49)$$

When z is large, $J_o(z)$ and $Y_o(z)$ behave like $\sqrt{2/\pi z}\cos(z - \pi/4)$ and $\sqrt{2/\pi z}\sin(z - \pi/4)$, respectively. Therefore, η_s can be written as

$$\eta_s(z) = \left(\frac{2}{\pi z}\right)^{1/2}\left(\frac{C_1 - C_3}{2}e^{i(z-\pi/4)} + \frac{C_1 + C_3}{2}e^{-i(z-\pi/4)}\right)e^{i(ly+\omega t)}. \quad (50)$$

The behavior of a modulated wave (amplitude varies slowly in space compared to the variations in the phase function) can be described through the simplified geometrical techniques of ray theory. If $P(x) = \sqrt{2/\pi z}$ and $Q(x) = z - \pi/4$, expression (50) represents a plane wave if

$$|(1/P)(dP/dx)| \ll dQ/dx$$

$$1/2z \ll 1.$$

Since Bessel functions $J_o(z)$ and $Y_o(z)$ behave like $\sqrt{2/\pi z}\cos(z - \pi/4)$ and $\sqrt{2/\pi z}\sin(z - \pi/4)$, respectively, when $z \geq 3\pi/4$, (50) can be regarded as a plane wave of the form $A(x, t)\exp(i\theta)$ and ray techniques can be applied. Therefore, the wavenumber and the frequency are given respectively by the gradient and the time derivative of the phase function; that is,

$$\theta_x = k,\ \theta_y = l,\ \theta_t = \omega. \quad (51)$$

Therefore, from (50) and (51) the wavenumber in the x direction and the phase speed on the shelf are given by

$$k_s(x) = \left\{\frac{\mu s^2}{h(x)}\right\}^{1/2} \quad (52)$$

$$c(x, t) = \left\{\frac{\omega^2 h(x)}{\mu s^2}\right\}^{1/2}. \quad (53)$$

When there is no friction,

$$c(x, t) = \left\{\frac{\omega^2 h(x)}{h_o(k_o^2 + l^2) + (fls/\omega)}\right\}^{1/2}. \quad (54)$$

Since the group velocity is given by

$$\mathbf{c_g} = \mathbf{c}^2\mathbf{k}/\omega, \quad (55)$$

the ray path can be determined from the real part of the expression below

$$y = \frac{l}{\sqrt{\mu s^2}}\int \sqrt{h}\, dx. \quad (57)$$

3. Results

a. Parameters

There are a relatively large number of parameters to vary in order to obtain a general description of the results of the model. These include the coastal depth h_1, the shelf edge depth h_2, the ocean depth h_o, and the shelf width a. The shelf slope s is dependent on some of these. Other physical constants are provided by the Coriolis parameter f and the shelf bed friction parameter r. Parameters of the incident wave include the frequency ω, the angle of incidence α, and the wavenumbers k and l, which are related to other parameters through the deep ocean dispersion relation. It is not practical to calculate the tidal response to the full range of all parameters, so in the present work, the parameters have been chosen to facilitate comparison with other published papers.

In particular, we shall consider shelves of width 150–300 km having a shelf edge depth of $h_2 = 120$ m and an ocean depth of $h_o = 5000$ m. Variations in shelf slope will therefore be expressed through a variation in coastal depth h_1 and shelf width. The Coriolis parameter f is given by $f = -1.0838 \times 10^{-4}\ \mathrm{s}^{-1}$, appropriate for 48°S latitude. Such parameters allow comparison with the earlier work of Webb (1976), Buchwald (1980), and Middleton and Bode (1987) for the Patagonian shelf. Effects of variation in the friction parameter r are also typical of earlier work and we again use the (unusual) definition of frequency units for ω as radians per day. Note that the M_2 tide has $\omega = 1.40509 \times 10^{-4}\ \mathrm{s}^{-1} = 12.14$ rad day^{-1}.

b. Results for the flat shelf model

As noted by Buchwald (1980) the main cause of resonance on a flat shelf occurs through the quarter-wave-oscillator resonance. In this situation the tidal crest, propagating to shore from the shelf edge where it has been driven by the external tide, reflects from the coast and propagates out to the shelf edge, arriving at a time so as to be exactly in phase with the deep ocean tide once again. Middleton and Bode (1987) extended this work to account for the effects of oblique angle of incidence.

c. Results for zero shelf friction

To facilitate interpretation of the effects of friction, it is first necessary to gain an idea of the response when the friction $r = 0$. One response ratio of interest is the ratio of coastal amplitude to that at the shelf break ($|\eta_c|/|\eta_o|$). In case of zero shelf friction this ratio is one-half of the ratio of the coastal amplitude to that of the incident Poincaré wave $|\eta_c|/I$. To simplify the presentation, it is assumed that $\alpha = 0$ for these calculations. In Fig. 2 the ratio $|\eta_c|/I$ is plotted as a function of frequency ω and coastal depth h_1 for two selected shelf widths, 150 and 300 km.

For the moderate width or narrow shelf the response increases with increasing frequency at constant h_1 as resonance is approached. It also increases as h_1 is reduced at constant frequency primarily as a consequence of continuity: As the tide flows shoreward on the shelf,

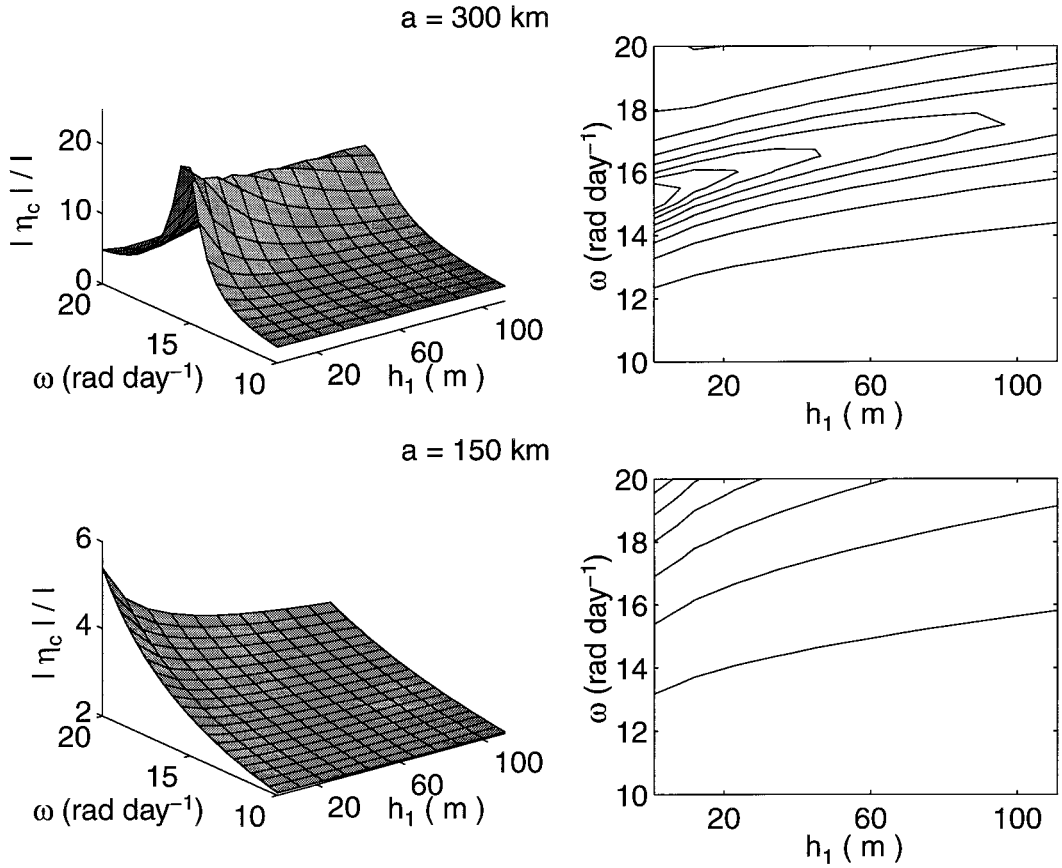

FIG. 2. Ratio of coastal amplitude $|\eta_c|/I$ to that of the incident Poincaré wave, I, as a function of ω and h_1 both for wide (300 km) and moderate width (150 km) shelves.

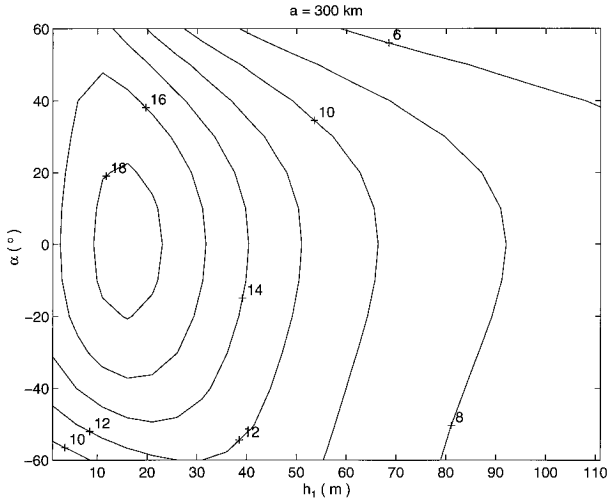

FIG. 3. Dependence of $|\eta_c|/I$ on h_1 and α when $\omega = 16$ rad day^{-1} for a shelf width of 300 km.

the shoaling depth demands a large surface elevation displacement. On a moderate shelf ($a = 150$ km), the tide travels too rapidly (has too large an overall wavelength at a given frequency) to allow resonance for the values used in Fig. 2. For the wider shelf ($a = 300$ km), resonance is seen to occur at frequencies of approximately 15 rad day^{-1} at $h_1 = 0$ m, increasing in frequency (but reducing in amplitude) as h_1 is increased to perhaps 18 rad day^{-1} when $h_1 = 100$ m.

To investigate the effects on the response of the joint variation of angle of incidence α and coastal depth h_1, calculations are plotted in Fig. 3 of the response $|\eta_c|/I$. In this case it is seen that (for the other parameters as given) the maximum response occurs at a coastal depth of some 15–20 m and with angles of incidence smaller than about 20°. There is little asymmetry in the response for left bounded ($\alpha > 0$) and right bounded ($\alpha < 0$) incident waves for smaller α although the asymmetry increases with $|\alpha|$. The results are quantitatively consistent with Middleton and Bode's (1987) Fig. 4a.

For any constant value of the coastal depth h_1, narrow shelves have a shorter ''quarter-wave'' wavelength for resonance and hence resonance occcurs at a higher frequency. This is shown clearly Fig. 4.

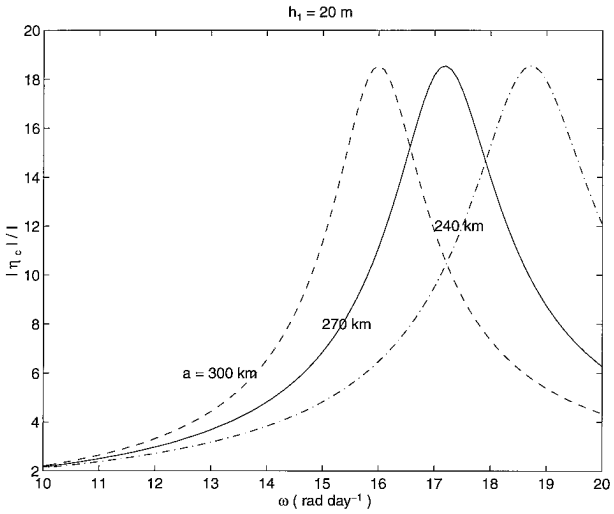

FIG. 4. Variation of $|\eta_c|/I$ with shelf width for a coastal wall depth of $h_1 = 20$ m.

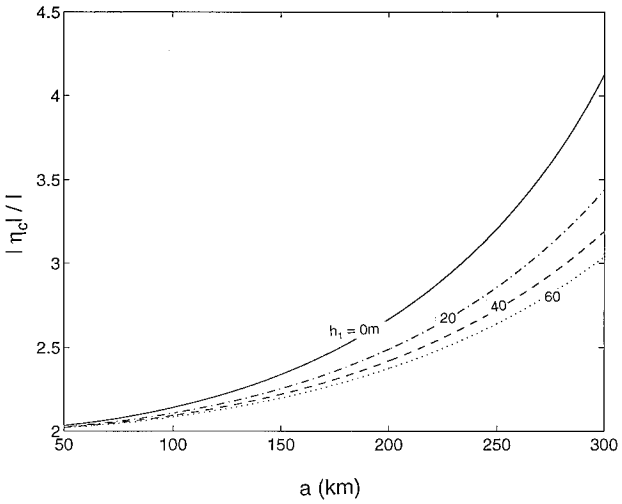

FIG. 5. Increase of M_2 tide with the increase of shelf width a and decrease of coastal wall depth h_1.

At the M_2 tidal frequency it is also instructive to determine the joint effects of shelf width a and coastal depth h_1. Figure 5 shows that $|\eta_c|/I$ increases with the increase of shelf width and the reduction in h_1. Wide shelves are more sensitive to a reduction in h_1 than narrow shelves.

Some general deductions can be made from the expression of phase speed (53). Phase speed decreases as the coast is approached because the water is shallower. Phase speed depends on l and is maximum when the wave is left bounded ($l < 0$). Therefore, resonance occurs at a lower frequency when $l > 0$ ($\alpha < 0$) than when $l < 0$ ($\alpha > 0$), which agrees with Middleton and Bode's (1987) results. Phase speed increases with the increase of h_1, so a shelf with a shallower coastal wall will resonate at a lower frequency (Fig. 2). In contrast to the flat shelf, for any particular angle of incidence the value of k_s depends on the sign of l.

Ray theory, when applicable, proves to be an extremely powerful tool, simplifying the solution of wave problems, usually stated in terms of partial differential equation, to an ordinary integration along rays. These characteristic curves are such that energy travels along this curve and the tangent at any point to this curve is in the direction of the group velocity. To apply the ray theory the amplitude of the wave should vary slowly in comparison to the variations in the phase function. This condition is automatically satisfied for large values of z when the roots of the Bessel function $J_o(z)$ are approximately those of $\cos(z - \pi/4)$. Since $J_o(z)$ has no complex zeroes, the positive zeroes of the equation $J_o(x) = 0$ are given approximately by $\beta_m = (m - 1/4)\pi$. This approximation is fairly good even for $m = 1, 2, 3, \cdots$ (Bowman 1958). So the theory of ray techniques can be applied when Re(z) is greater than $3\pi/4$. Figure 6 shows the minimum value of Re(z) as a function of h_1 and h_2, in other words as a function of slope (since the shelf width is constant). We see that z increases with the decrease in slope and a narrow shelf needs more gentle slope than a wide shelf to apply this theory. It also shows ray theory can be applied to shelves with a slope of the order of 10^{-4}. This value of z can be obtained for any width of shelf.

Figure 7 shows shelves having the same slope have a different ray path depending on the depth of the coastal wall. This statement is true both for wide and moderate width shelf.

d. Results for nonzero shelf friction

Figure 8 shows the response on a wide and moderate width shelf as a function of h_1 and ω when bottom friction ($r = .001$ m s^{-1}) is introduced. Comparing Fig. 8 with Fig. 2, it is clear that responses are reduced below those that occur for no friction at all frequencies. The reduction in response is greater on a wide shelf and is maximum near resonant frequency. Friction is more effective in shallower water so the response increases with increase of h_1.

Since resonance at the M_2 frequency occurs on a wide shelf (350 km), the reflection coefficient amplitude of the response on a wide shelf ($a = 300$ km) is shown in Fig. 9. The ratio $|R|/I$ changes with h_1 and it is minimum (but nonzero) at the resonant frequency, indicating that a small portion of the incident wave energy reflects back to the deep ocean, and maximum energy is absorbed on the shelf. Even at resonance those slopes with different coastal wall depths do not absorb the same amount of incident energy. Depending on the friction a particular slope absorbs maximum energy. In Fig. 9 we see that, when friction is $r = 0.001$ m s^{-1}, maximum energy is absorbed when the coastal depth is around 20 m.

The variation with bottom friction of the response and reflection coefficient amplitudes for three different

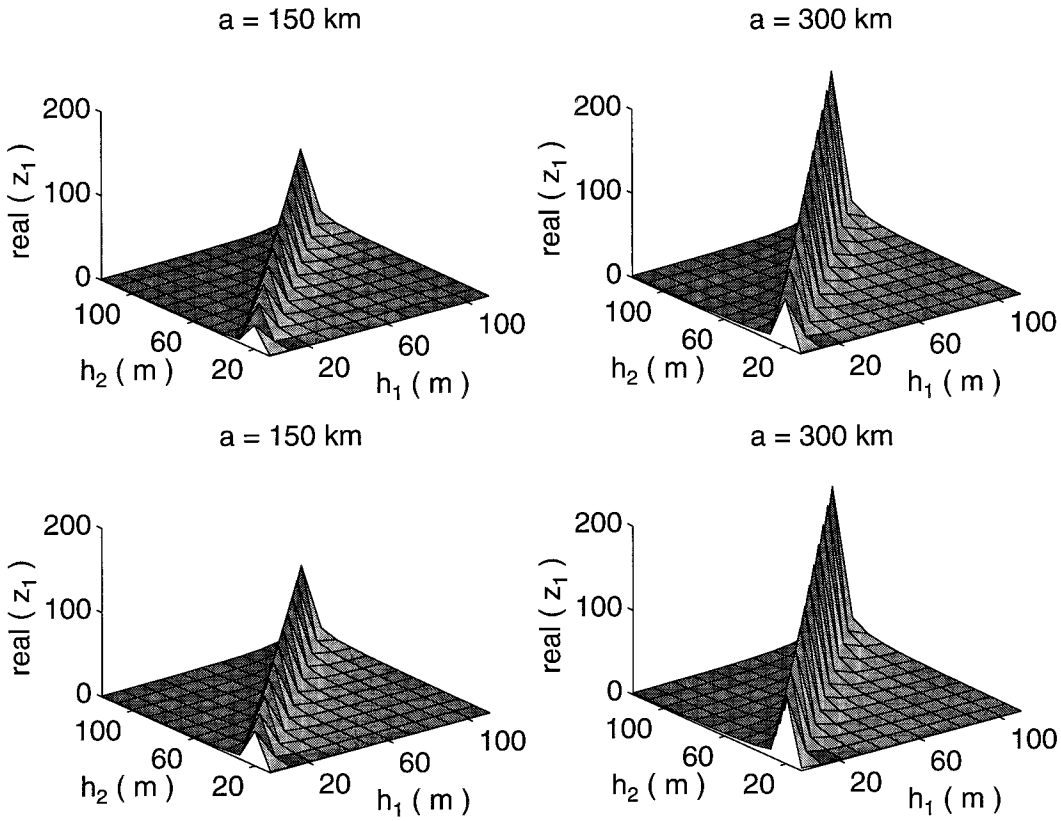

FIG. 6. The real part of z_1 as a function of h_1 and h_2 on a moderate width (a = 150 km) and wide (a = 300 km) shelf. The upper panels have zero friction, and the lower panels have friction r = .001 m s^{-1}.

slopes at their resonant frequencies are given in Fig. 10. Bottom friction is a force/unit area, so an increase of friction coefficient has more impact on a shelf with smaller coastal wall (and hence shallower water depth) than a larger. Therefore, with the increase of friction the response ($|\eta_c|/I$) decreases at a faster rate for h_1 = 20 m than for h_1 = 60 m. Thus when friction is more than a critical value r = 0.0008 m s^{-1} (this value depends on the depth at shelf break) a greater depth at the coast gives higher amplification. Buchwald (1980) mentioned that almost all incident tidal energy will be absorbed at a particular friction, which depends on the shelf parameters. It is found here that this value also depends on h_1.

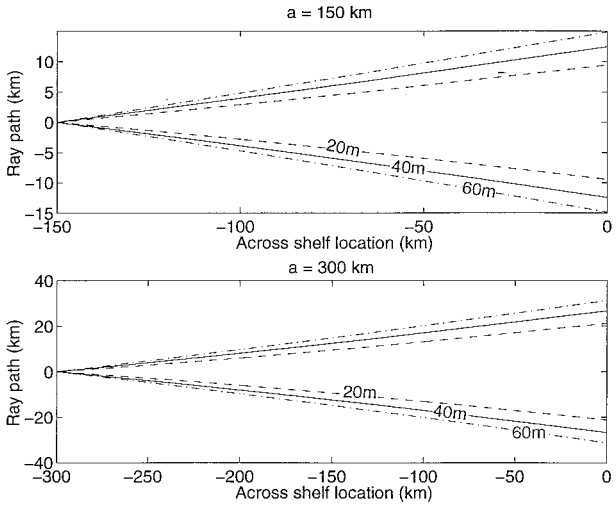

FIG. 7. The ray path on a moderate width and wide shelf when slope is 10^{-4} and friction is zero for selected cases of coastal wall depth.

Due to presence of the bottom friction tidal energy is dissipated on the shelf. The mean rate of tidal energy dissipation is equal and opposite to the mean tidal energy flux (45). Since the amplitude of the reflection coefficient depends on the slope, the dissipation is different for different h_1. For any particular slope it is maximum when $\alpha = 0°$ (Fig. 11).

The dissipation rate of the M_2 tide is shown as a function of the friction coefficient r in Fig. 12. Dissipation increases with the increase of friction but decreases with the increase of h_1. In case of the M_2 tide more energy will be absorbed on a shelf with small coastal depth.

Figure 13 shows the dependence of the magnitude and phase of the coastal to shelf break response on h_1 for a normal incident wave. The peak at ω = 17.0 rad

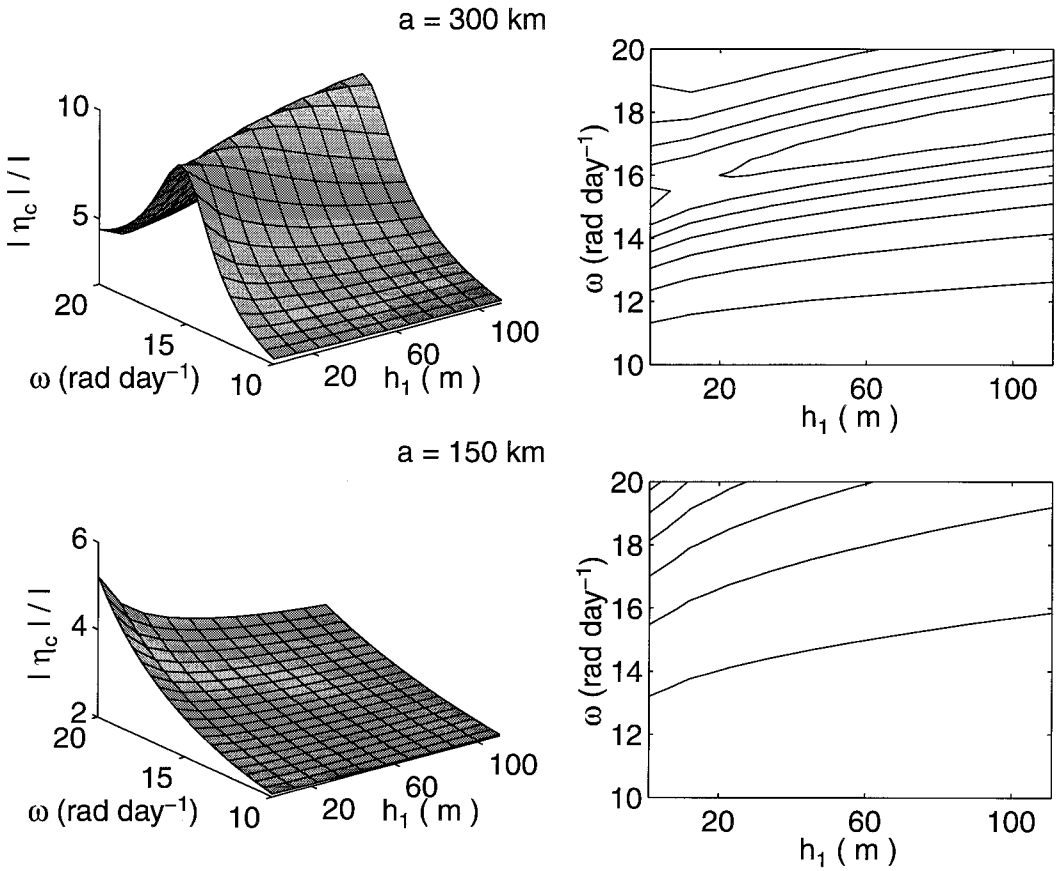

FIG. 8. Response amplitudes on a wide and moderate width shelf, given as a function of frequency ω and coastal wall depth h_1.

day^{-1} (h_1 = 60 m) is larger than that at ω = 16.5 rad day^{-1} (h_1 = 40 m), which is itself larger than that at ω = 16.0 rad day^{-1} (h_1 = 20 m). If the frequency is less than the resonant frequency, a smaller depth at the coast leads to higher amplification. The situation is reversed

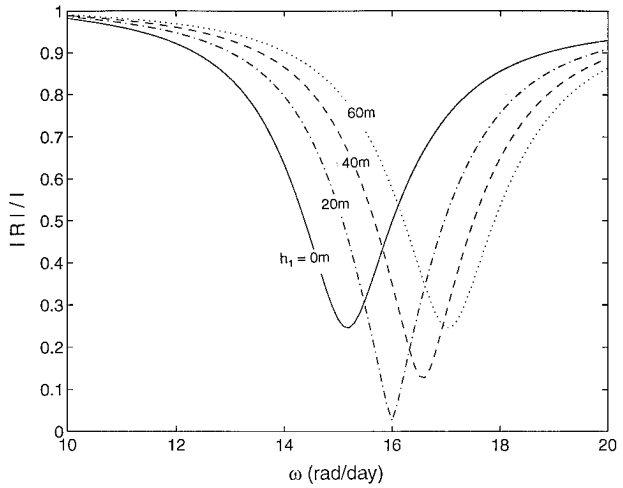

FIG. 9. Reflection coefficient amplitudes on a large shelf as a function of frequency and coastal wall depth.

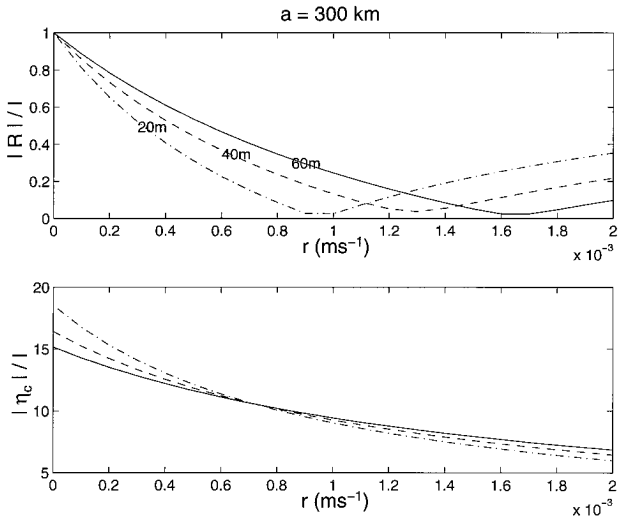

FIG. 10. Response and reflection coefficient amplitudes as a function of friction for three different values of h_1 at their resonant frequencies.

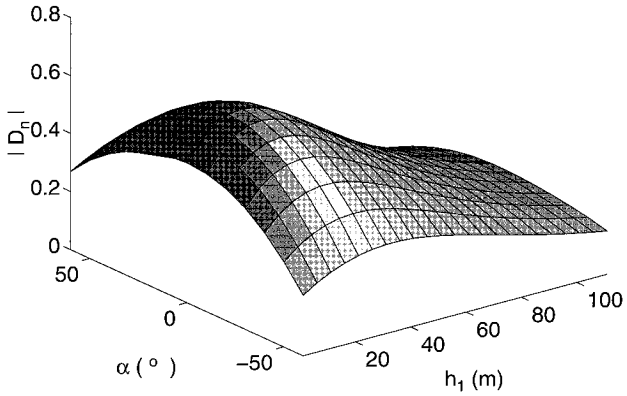

FIG. 11. Normalized dissipation $|(D_n)|$ for $a = 300$ km and different coastal wall depths h_1 and different values of angle of incidence α.

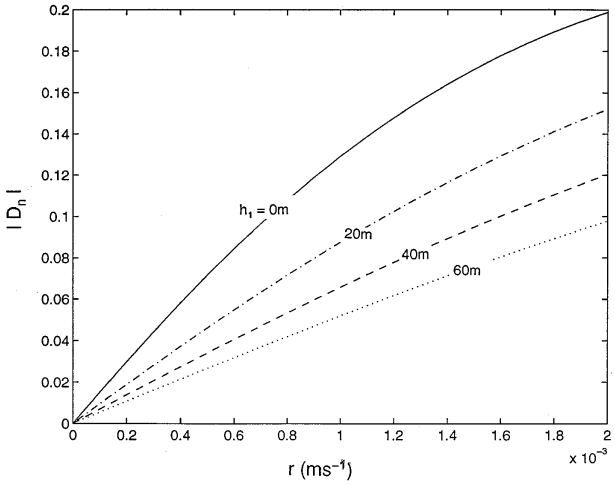

FIG. 12. Normalized dissipation ($|D_n|$) of the M_2 tide as a function of friction coefficient r and the coastal wall depth h_1.

for frequencies higher than the resonant frequency. The phase of the ratio depends markedly on h_1 near the resonant frequency.

The across-shelf structure and phase of the M_2 tide compared to that at the shelf break $[\eta_s(x)/\eta_0(0)]$ are shown as a function of h_1 for three different angles of incidence ($\alpha = 60°, 0°, -60°$) in Fig. 14. In the Southern Hemisphere $f < 0$, so Kelvin waves travel with the coast to the left of the direction of propagation. The influence of Kelvin wave type dynamics makes the amplitude higher in the case of a left bounded wave. Figure 14 clearly shows that the left bounded wave has higher amplitude than the right bounded wave, and the effect of h_1 is larger on the left bounded wave. The phase change across the shelf depends more on the depth of the coastal wall h_1 than on the angle of incidence. For a shelf of width 300 km, the phase changes for a shelf with 1-m coastal wall are 22.4° ($\alpha = -60°$), 23.3° ($\alpha = 0°$), and 24.3°($\alpha = 60°$), respectively. By contrast, the phase change for three different depths at the coast are 24.3° ($h_1 = 1$ m), 18.8° ($h_1 = 11$ m), and 15.6° ($h_1 = 21$ m) when $\alpha = 60°$.

The angle of incidence strongly affects the velocity ratio $|v/u|$ (Middleton and Bode 1987) but the ratio depends on h_1 as well. This ratio is constant when $\alpha = 0$ ($|v/u| = |f|/|\sigma|$). Since the constant does not depend on h_1, shelves with different coastal wall depths can have the same velocity ratio across the shelf when the wave is incident normally. When waves are incident at an angle, the ratio depends on h_1. Near the coast it depends strongly on h_1. In case of a left bounded wave, this ratio becomes almost zero near the coast. The position of the minimum ratio $|v/u|$ lies closer to the coast for smaller values of h_1. Any variation of h_2 does not make much difference. Figure 15 shows these results are true for any type of shelf, that is, wide or moderate width.

Ray theory can be applied to shelves with different slopes to determine the effects of friction. From Fig. 16 we see friction is more effective on a shelf with a small coastal wall. Refraction of the ray path from the shelf break to the coast increases with the increase in h_1,

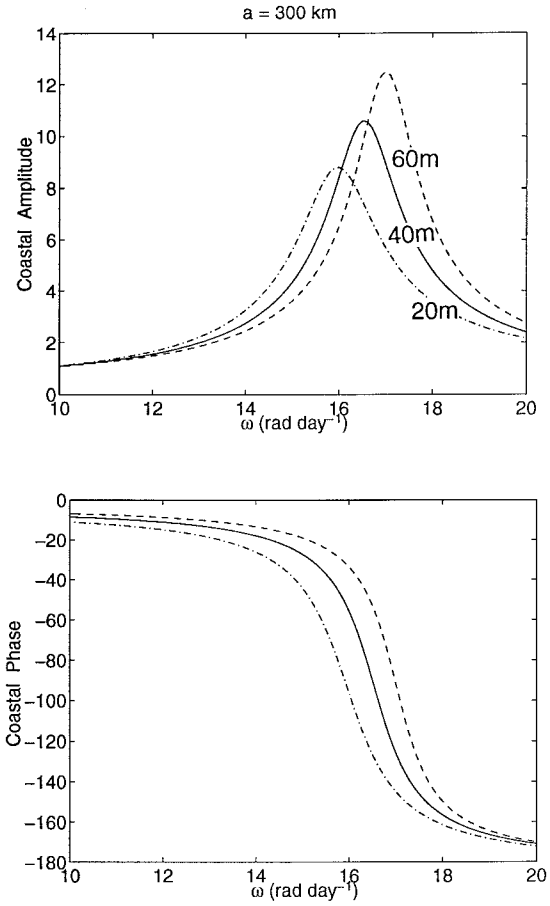

FIG. 13. Magnitude and phase of the coastal amplitude ratio as a function of frequency for three different depths at the coast.

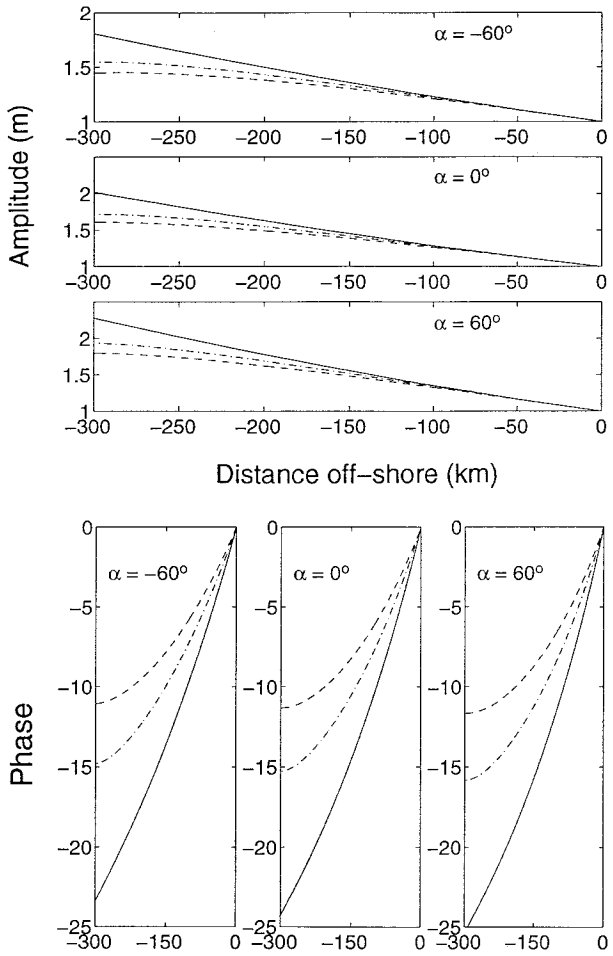

FIG. 14. Across-shelf structure and phase of the M_2 tide compared to that at the shelf break for three different angles of incidence and for three different coastal depths. Solid line represents zero depth, where dash–dot line represents 20-m depth and dash line represents 40-m depth at the coast.

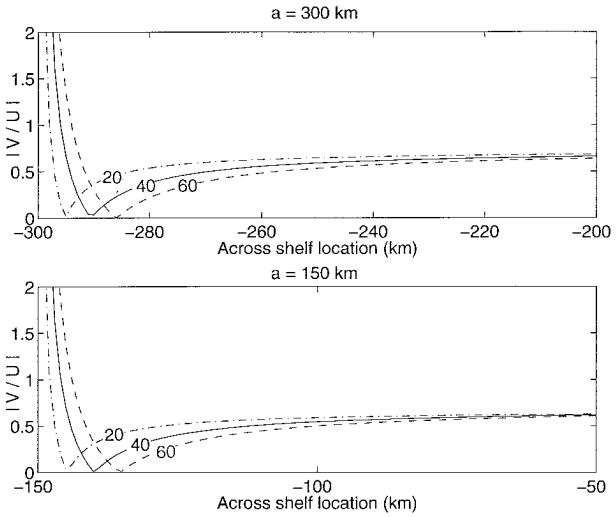

FIG. 15. Velocity ratio $|v/u|$ of the M_2 tide near the coast when the angle of incidence is 60° and depths at the coast are 20 m, 40 m, and 60 m respectively.

whereas friction reduces the refraction. Also the refraction increases as the angle of incidence increases (not shown).

It is useful to compare the results of this model with those of Church et al. (1985). These authors used Battisti and Clarke's (1982a) model to predict the currents in the central Great Barrier Reef. In their model l was assumed to be complex and estimated from the coastal data. They agreed that estimation of l from noisy coastal data was difficult and incorrect estimation of l leads to an error in the result. In the present model this problem has been avoided by calculating l from the deep water values. Clarke and Battisti (1981) have shown that l is independent of x. So equating the negative value of l_r (note the different terminology used for the phase lag) given in Church's (1985) paper to our parameter l allows the angle of incidence to be found. Using these values along with other parameters used by Church (1985), the tidal amplitude and cross-shelf velocity across the shelf has been plotted in Fig. 17, and this figure is comparable with Fig. 4 in Church's paper.

Finally in Fig. 18 we provide a quick summary of the effects of coastal wall depth at three different shelf widths. Even a small value of h_1 (20 m) can make a large difference in coastal response for all depths. Since the values of h_1, h_2, a, and slope are not independent of each other it is difficult to directly ascribe effects to one parameter only, however, it is clear that even a small value of h_1 can make a large difference in response.

4. Discussion

A simple analytical model of tidal flow onto a continental shelf is formulated using a sloping shelf ba-

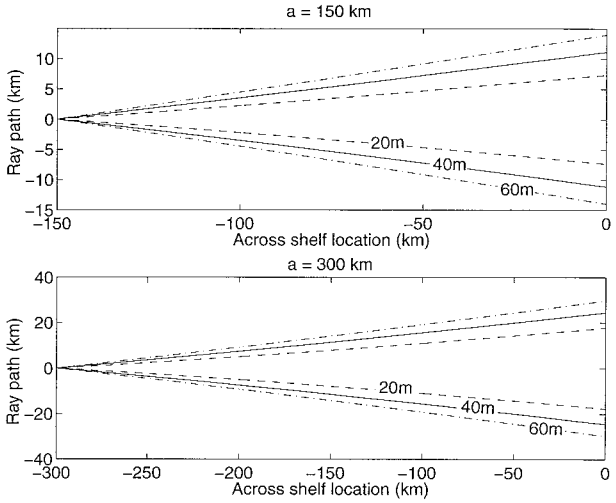

FIG. 16. Ray path on a moderate width and wide shelf when slope is 10^{-4} and friction is 10^{-3} m s^{-1} for selected values of the coastal wall depth h_1.

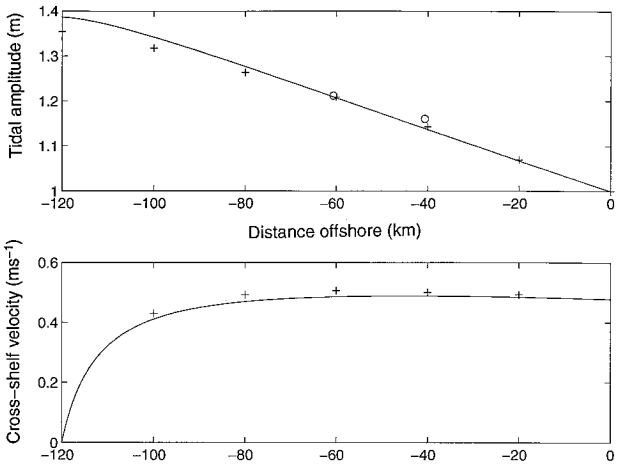

FIG. 17. The computed tidal amplitude and cross-shelf velocity of the M_2 tide in the Great Barrier Reef as a function of distance from the coast. The solid line represents our calculation, while the plus symbol indicates tidal heights computed by Church and the open circle indicates the observed tide.

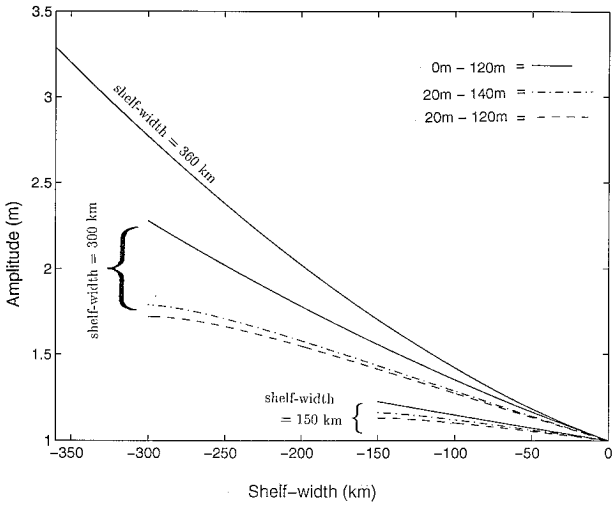

FIG. 18. Across-shelf structure of M_2 tide on three different width shelves for different combinations of depths at the coast and at the shelf break.

thymetry on a shelf that is predominantly straight and whose profile is independent of longshore position. The adjacent deep ocean has constant depth, while at the coast the water depth is considered to be, in general, nonzero. This bathymetry allows a full matching of ocean and shelf flows in cases where the shelf flows may be affected by bottom friction. The complete solution, comprising Bessel functions of the first and second kind, allows a consideration of flows that are obliquely angled and partly reflected from the coast.

The dependence of the tidal response on the shelf has been evaluated for a range of parameters and a comparison made with earlier theoretical studies. Specific objectives have been to determine the influence of the coastal wall, and the angle of incidence for both very wide (300 km) and moderate (150 km) shelf widths. At the larger shelf widths, resonance is approached and the shelf response becomes large.

In the case of zero bottom friction, for frequencies lower than the resonant frequency, an increase in coastal depth results in a reduction in sea-level amplitude at the coast. For moderate width or narrow shelves, the response always decreases with increase in coastal depth. This situation is reversed for frequencies exceeding the resonant frequency. The resonant frequency depends on both the angle of incidence and the coastal wall depth, with the resonant frequency increasing with coastal depth. An asymmetry is evident between left bounded waves and right bounded waves, with waves traveling in the same direction as Kelvin waves having a larger response in general, but also being more easily affected by changes in coastal depth.

Bottom friction reduces the response on both wide and moderate shelf widths, but the reduction is most evident near resonance on a wide shelf. The overall energy dissipation rate is also found to depend on the coastal depth, with dissipation decreasing as coastal depth increases.

Comparison of our results with those of Church (1985) shows that the estimation of alongshore gradients from noisy coastal data can be avoided by determining alongshore wavenumbers from the angle of incidence and the deep-ocean parameters.

Acknowledgments. This work was supported by the Australian Research Council and by an Australian Postgraduate Award to P. Das.

REFERENCES

Battisti, D. S., and A. J. Clarke, 1982a: A simple method for estimating barotropic tidal currents on continental margins with specific application to the M_2 tide off the Atlantic and Pacific coasts of the United States. *J. Phys. Oceanogr.*, **12,** 8–16.

——, and ——, 1982b: Estimation of nearshore tidal currents on nonsmooth continental shelves. *J. Geophys. Res.*, **87,** 7873–7878.

Bowman, F., 1958: *Introduction to Bessel Functions.* Dover, 135 pp.

Buchwald, V. T., 1980: Resonance of Poincaré waves on a continental shelf. *Aust. J. Mar. Freshwater Res.*, **31,** 451–457.

Clarke, A. J., 1991: The dynamics of barotropic tides over the continental shelf and slope (review). *Tidal Hydrodynamics,* B. B. Parker, Ed., John Wiley, 79–108.

——, and D. S. Battisti, 1981: The effect of continental shelves on tides. *Deep-Sea Res.*, **28A,** 665–682.

Church, J. A., J. C. Andrews, and F. M. Boland, 1985: Tidal currents in the central Great Barrier Reef. *Contin. Shelf Res.*, **4,** 515–531.

Koblinsky, C. J., 1981: The M_2 tide on the west Florida shelf. *Deep-Sea Res.*, **28A,** 1517–1532.

Middleton, J. H., and L. Bode, 1987: Poincaré waves obliquely incident to a continental shelf. *Contin. Shelf Res.*, **7,** 177–190.

Webb, D. J., 1976: A model of continental-shelf resonances. *Deep-Sea Res.*, **23,** 1–15.